International Journal of Current Engineering and Technology
E-ISSN 2277 – 4106, P-ISSN 2347 – 5161

Available at http://inpressco.com/category/ijcet

Research Article

Preliminary Study of Printing Optical-Based Materials using Aerosol Jet Deposition Process

Aleksandra Fortier[#*], Max Tsao[#], Nick D. Williard[^], Yinjiao Xing[!] and Michael G. Pecht[!]

[#] University of Dayton Research Institute and The Air Force Research Laboratory, Wright-Patterson Air Force Base, OH 45433, USA
[^]1430 Enclave Pkwy Schlumberger, Houston, TX 77077, USA
[!]Mechanical Engineering Department, Center for Advanced Life Cycle Engineering, University of Maryland, College Park, MD 20742, USA

Received 15 March 2018, Accepted 19 May 2018, Available online 23 May 2018, **Vol.8, No.3 (May/June 2018)**

Abstract

This work examines the printing of optical-based materials using aerosol jet printing (AJP), an additive manufacturing process. Deposition of optical-based materials using the AJP process has potential to be applied in the fabrication of embedded fiber optic Bragg grating sensors. Made from silica (SiO_2), fiber optic Bragg grating sensors are small, lightweight, and chemically inert, making them suitable for a variety of applications. This study examines the preparation and deposition of a newly developed silica-based printing ink. The results of the printing method, the impact of various printing and processing parameters on the deposition quality and microstructure, light reflectivity, scanning electron microscope (SEM) images, and content analyses of the deposited layers are presented. The results show uniform printed layers and demonstrate the capability of the AJP method as well as the newly developed silica-based ink to print high-quality commercial optical-based materials. The focus of this study is on the process/ optical material property interaction only; the printing of actual functional sensors on components and testing them will be discussed in later studies and is beyond the scope of this paper.

Keywords: *Aerosol 3D jet; additive manufacturing; optical fibers; fiber Bragg grating sensors; silica-based printing ink.*

Introduction

Over the past several decades, electrical sensors have been the main technology for measuring physical and mechanical variations in components. However, in an effort to eliminate several of their limitations, such as transmission loss and susceptibility to electromagnetic interference (noise), that make their usage challenging or impractical in many applications, special attention has been given to fiber-optic sensing technologies [M. M. Werneck *et al*, 2013 – K.O. Hill, 2000]. Optical-based fibers are small, lightweight, and chemically inert. They use light transmittance rather than electricity for measuring various phenomena; therefore, they can be embedded in high-voltage and potentially explosive locations [M. M. Werneck *et al*, 2013, G. Meltz *et al*, 1989 – B. Gwadu *et al*, 2004]. One of the most commonly used optical sensors is fiber Bragg grating (FBG). An FBG measures local temperature and strain variations based on shifts in light wavelength [A. Othonos *et al*, 1999 – F. Julic *et al*, 2009]. Due to their small size and ease of installation, FBG optical fibers can find use in a variety of industries including aerospace, biomedical, automotive, construction, and petroleum [M. M. Werneck *et al*, 2013, www.wikipedia.com 2016]. With more technological advances, the need for "smart" structures and materials that can provide real-time information to mitigate sudden system failures increases, and efficient fabrication methods of FBG sensors are essential. To implement FBG sensors in a variety of applications, several challenges need to be overcome. Specifically, FBG sensors are prone to breakage when placed in small-size electronics or lithium-ion (Li-ion) battery cells that require a vacuum-sealed environment to ensure proper functionality. Li-ion batteries have been adapted to many electronic devices, and although they are often the battery of choice they still suffer from significant reliability issues such as electrode stress or cracking, dendrite growth as a result of lithium plating, internal cell defects, and overheating that leads to thermal runway and fire [A. Patil *et al*, 2008].

Embedding FBG sensors inside battery cells can drastically improve Li-ion cell reliability over time. Because optical fibers are drawn on the assembly line, FBGs are typically "inscribed" or "written" onto the core of the optical fiber by two of the most commonly used processes: interference or masking with femtosecond laser and other laser-based technologies [C. Liao *et al*, 2013].

*Corresponding author's ORCID ID: 0000-0001-7612-6572
Email: drafortier@gmail.com
DOI: https://doi.org/10.14741/ijcet/v.8.3.16

To simplify the process of embedding FBG sensors into battery cells and other miniature devices, optical-based materials can be printed using an aerosol 3D jet printing (AJP) process. Until now, literature reports only few printing methods for optical (glass) -based materials: a fused deposition molding approach in which soda lime glass is heated to around 1,000 °C, a manual wire feeding approach in which a glass filament is melted using a laser beam, and a stereolithography process at resolutions of a few tens of micrometres to deposit high-quality fused silica glass via heat treatment using photocurable silica nanocomposite as starting material [J. Klein *et al*, 2015 – F. Kotz *et al*, 2017]. Other processes like inkjet printing, selective laser melting or sintering of glass powders have so far limited their capability to depositing only non- reflective glass components [G. Marchelli *et al*, 2011 , - A. Sukeshini *et al*, 2010]. This paper provides preliminary results with insight towards future printing of fiber optic sensors using the AJP process. Preparation of SiO_2-based ink, methods for printing, the impact of various printing and processing parameters on the deposition quality and microstructure, light reflectivity, scanning electron microscope (SEM) images, and content analyses are presented and discussed. The focus of this study is on the process/optical material property interaction only; the printing of actual functional sensors on components and testing them will be discussed in later studies and is beyond the scope of this paper.

Experimental Approach

Deposition System

Material deposition was carried out by a commercially available Optomec Aerosol Jet system, which was formerly known as M³D (Maskless Mesoscale Material Deposition). Aerosol Jet is an environmentally benign, room-temperature-operated, software-driven additive manufacturing process, and its intended use is to reduce the overall size of electronic systems by using nano-inks to print fine-featured circuitry and embedded components. The resulting functional electronics can have line widths and pattern features ranging from below 10 µm to as large as several millimeters because Aerosol Jet deposition uses an innovative aerodynamic focusing technology [20]. The system can directly deposit a wide range of commercial and custom electronic materials, including conductive nanoparticle inks, insulators, polymers, adhesives, dopants, etchants, and even biological materials on virtually any planar or non-planar substrate. The deposition system is composed of a deposition head, ultrasonic and pneumatic atomizers, and a process control module (PCM). Deposition patterns are typically designed using computer-aided design (CAD) software and converted into .dxf files (compatible with the printing system) using VMTools (VMT), which is an integral part of the system. The Aerosol Jet processes the material using liquid ink of a desired composition placed into an atomizer, creating a dense aerosol of 1–5-µm droplets. The aerosol is carried by a gas flow to the deposition head. The Aerosol Jet process begins with a mist generator that atomizes a source material. Particles in the resulting aerosol stream can then be refined in a virtual impactor and further treated on the fly to provide process flexibility. Figure 1a shows the three-step deposition process. Within the deposition head the aerosol is focused by a second gas flow and the resulting high-velocity stream is deposited on the substrate, creating the desired pattern. Aerosol Jet comes with adjustable stand-off distance (Figure 1b) with five-axis rotation that can map the surface and can be positioned at a large height above any surface to be coated. This feature allows printing over a variety of conformal surfaces. Further system details (e.g., motion, substrate positioning, camera alignment) can be found in the literature [A. Suksheni *et al*. 2010].

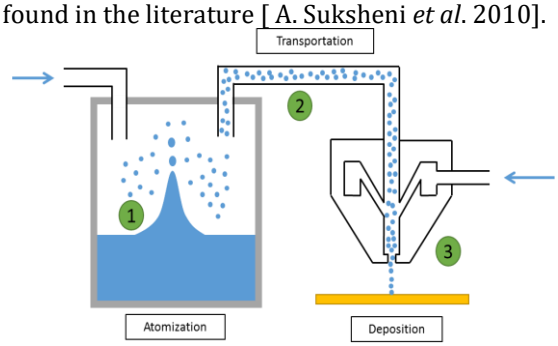

(a)

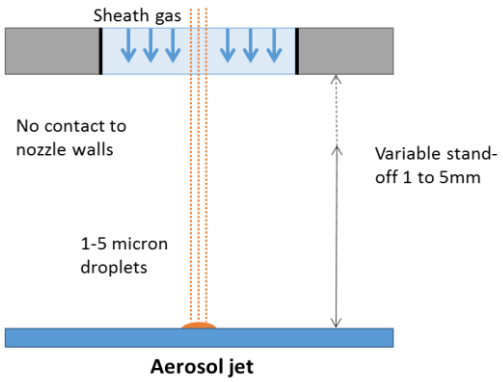

(b)

Figure 1 Aerosol 3D jet deposition technology: (a) schematic of the three-step deposition process (b) adjustable stand-off distance [J. Klein *et al*. 2015].

Properties of Optical-based Materials and Silica-ink Preparation

Material selection was based on the ultimate goal of printing fiber optic FBG sensors. Some requirements are based on the material's need to reflect light and ability to be deposited with 3D structure using aerosol jet printing. 3D structures can be formed using *in-situ* ultraviolet (UV) light during printing with the Aerosol Jet, therefore, the material content should be photopolymer-based so that it can be instantly cured

with the UV light. Based on the listed requirements, four Norland (NOA) optical-based adhesives (NOA 65, 71, 74, 84) were selected for investigation with variable refractive index and viscosities. A summary of all material properties used in this study is presented in the results section.

Ultimately, the goal of the printed material is to closely resemble properties of the commercial FBG sensors, which are made from pure SiO_2. SiO_2-based printing ink is not commercially available and was custom made for the first time in this study using SiO_2 powder with 200-nm particle size and solvents. The solvents can be any optical-based photopolymer in this study we developed a custom. The reason custom ink was developed in the lab was to achieve mostly silica content in the ink since commercial FBG sensors are made from pure silica. If only optical based solvent was used for printing then the content is not pure silica. Patent is pending on the ink development. Particle size was selected based on the specifications for commercially available ink solutions (Ag, Cu, Au, Ni, etc.), and typically a powder size between 5 and 200 nm is recommended for the Aerosol 3D Jet tool [www.optomec.com, 2016]. Other additives to the solution can help reduce particle agglomeration. One example is terpineol ($C_{10}H_{18}O$), which has been shown in our experiments to alter viscosity of the silica-based ink if necessary. Once the solution was prepared, it was magnetically stirred for 2 h before deposition. The substrate for all depositions in this paper was a glass slide. Viscosity measurements of the inks were obtained using a Rheolab QC (Anton-Paar) rheometer. Refractive index measurements were obtained using a Schmidt+Haensch digital refractometer, model DSR-λ.

Deposition Process Parameters:

A deposition head of 200 µm was used for all material depositions except for NOA 65 where a 300-µm deposition head was more suitable due to the high viscosity of this material. Each sample was deposited with a width of 28 mm and 50 rows at the 50 µm feature trace width and a servo stepping resolution of 10 µm. Three layers were deposited, layered on top of one another, for each material with curing of each layer immediately after deposition using UV 365-nm-wavelength light. The printing pattern followed for each sample is shown in Figure 2.

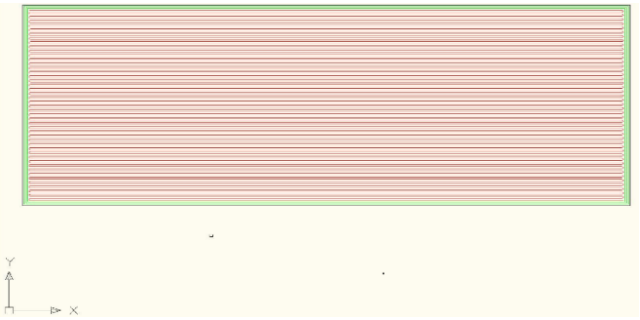

Figure 2 Printing pattern for each material deposition in this study using Aerosol Jet

Substrate travel speed was set to 7 mm/s, and the stand-off distance between the nozzle and the substrate was set to approximately 4 mm. The optimized settings for atomization flow rate, virtual impactor flow rate, and sheath flow rate in cubic centimeters per minute (ccm) are listed in Table 1.

Table 1 Deposition settings for each material deposition

Material	Atomizer Flow Rate (ccm)	Sheath Flow Rate (ccm)	Virtual Impactor Flow Rate (ccm)
NOA 65	1,400	5	1,250
NOA 71	1,600	15	1,450
NOA 74	710	15	675
NOA 84	875	10	860
Custom SiO_2-based ink	1,400	5	1,200

Surface, Content Analyses, Mechanical Testing, and Light Reflection Inspection

The surface of each deposited sample was sputtered with a very thin layer (~500 nm) of gold (Au) so that the samples surface could be analyzed using a scanning electron microscope (SEM), operated at 20 kV and 30 pA. The composition of each sample was inspected by energy dispersive spectroscopy (EDS) function of the SEM system. All measurements were performed with an accelerating voltage of 15 kV, a probe current of 1150 pA, and a 30-s acquisition time. A digital profilometer was used to estimate the final thickness of each deposited sample. Mechanical testing for the properties of each material was performed using Instron and Micro hardness testers. Each sample was tested for light reflectivity because this study will potentially be applied to the fabrication of FBG sensors. Figure 3 shows the set-up for testing the ability of the deposition to reflect light and the quality of the reflection.

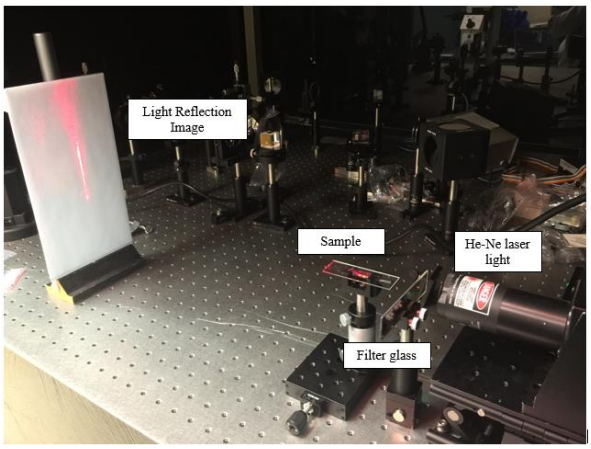

Figure 3 Light reflection test set-up

The light is generated using helium-neon (He-Ne) laser light positioned parallel with respect to the sample. If

the reflected image on the vertical white surface (as shown in Figure 3) is uniform and narrow that means the deposited sample has no defects and the deposition is uniform as shown in Figure 3. In the results section, poor quality samples will be also shown with scattered light reflection just for comparison.

Results and Discussion

Initially, the mechanical properties of each material were examined. Table 2 summarizes the measured modulus of elasticity, tensile strength, elongation at failure, hardness, and deposited thickness values. The results show that the newly developed SiO_2-based ink has increased strength and hardness but is more brittle compared to commercial optical-based materials. Increased brittleness is due to increased SiO_2 content, which is a positive result that furthers the study's goal of mimicking commercial FBG fibers made from pure SiO_2. Also, it is evident that the newly formed SiO_2-based ink has some of the same properties as the commercial Norland materials, however, the silica content distinguishes this ink. Silica plays a vital role in the content of the newly formed ink based on the properties measured in Table 2. Visual inspection and hardness measurements also confirm that silica increases the strength of the photopolymer solvent and gives that glassy finish once UV curing is completed.

The refractive index for each material was measured at room temperature, and the distribution curves over different wavelengths in the range between 400 and 900 nm are presented in Figure 4. The newly developed SiO_2-based ink has an average refractive index value of 1.50 with a value of 1.51 at around 400 nm wavelength (Fig. 4). These refractive index values are close to those of pure silica from which FBG sensors are made [M. Werneck *et al*, 2013]. The rest of the optical-based materials showed refractive index values at a wavelength of around 400 nm, which is close to the reported literature [www.Norlandproduct.com], and for the first time additional refractive index values at different wavelengths are reported in Figure 4 for these materials. The refractive index values of SiO_2-based ink, NOA 74, and NOA 65 are close to each other in the range between 1.50 and 1.53 where NOA 71 approaches 1.54 values and NOA 84 shows very low refractive index values nearing 1.45.

Viscosity is an important property to consider because it helps the Aerosol Jet printer deposit material. The silica content of NOA 84 doubled its original viscosity (average value of 45 CPS, Fig. 5). Figure 5 shows the viscosity of each material. The SiO_2-based ink has an average value of 86 CPS. The addition of terpineol can alter the viscosity of the ink 65 CPS (Fig. 5). Thus, terpineol can play a vital role by adjusting the viscosity in future work, whereby increasing the amount of silica and decreasing the amount of solvent will be necessary in order to mimic the original properties of FBG optical sensors with printing. The viscosity of the rest of the materials was as follows: NOA 71 and NOA 74 measured in the range between 100 CPS and 200 CPS; NOA 65 was the most viscous at around 1000 CPS; as a result, larger deposition heads were required than the other materials.

Table 2 Properties and characteristics of deposited materials in this study

Material	Thickness (µm)	Modulus of Elasticity (PSI)	Tensile (PSI)	Elongation at Failure	Hardness (Shore D)
NOA 65	35	20,000	1,500	80%	50
NOA 71	71	55,000	1,300	43%	86
NOA 74	37	2,900	217	10%	30
NOA 84	22	1,140	649	57%	55
Custom SiO_2- based ink	85	11,400	1,950	30%	75

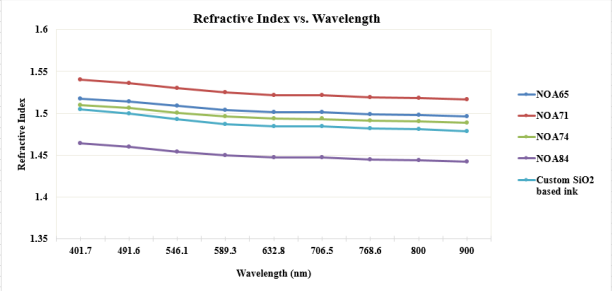

Figure 4 Refractive index distribution over different wavelengths for each material.

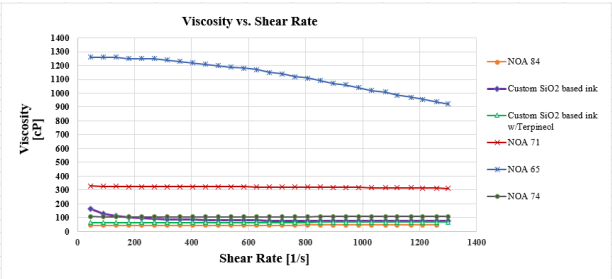

Figure 5 Viscosity vs. shear rate for each material.

Surface quality and elemental content was inspected for each material deposition (Fig. 6). Figures 6a, 6c, and 6i show uniform surface and very sharp edge definition for NOA 65, NOA 71, and custom SiO_2-based ink materials, whereas Figs. 6e and 6g show an uneven surface with over-sprayed edges and mist of particles on the side for NOA 74 and NOA 84. EDS images for

elemental content of all commercial materials show that the typical elements are carbon (C), oxygen (O), and sulfur (S) (Figs. 6b, 6d, 6f, and 6h). A strong Si peak is present in the newly developed silica-based ink (Fig. 6j), which proves that NOA 84 solvent absorbs Si powder very well and even after atomizing the material and depositing with Aerosol Jet the silica content is retained. It should be noted that the Au peaks in the EDS images of Fig. 6 are a result of a very thin sputtered layer on each sample surface in order for the surface topography to be examined under the SEM and this layer should be omitted.

The material depositions presented in this study using various properties, viscosity, and refractive index values provide a fundamental understanding of how material properties interact with the AJP process and under what parameters a combination of high-quality depositions can be achieved. The fluid contact angle and its interaction with the surface of the substrate is also necessary for solid, uniform deposition with clear edge definition, as shown in Fig. 6 for cases of NOA 65, NOA 71, and custom SiO_2-based ink. Viscosity allows the fluid to be effectively atomized, delivered to the deposition head in droplet form, and deposited in a uniform layer, thus, viscosity is interrelated with the fluid's contact angle and surface tension. This finding is evident from the low overall quality deposition shown in Fig. 6g for NOA 84, which has a viscosity of 45 CPS, and the high-quality deposition shown in Fig. 6i for the custom SiO_2-based ink, which has an increased viscosity of 86 CPS. The main parameters that were adjusted for optimization of material depositions in this study included: sheath flow rate, virtual impactor flow rate, atomizer flow rate, substrate travel speed, substrate/nozzle standoff distance, deposition head diameter, and trace width. However, atomization rate was the key factor in this process because it can control the amount of fluid delivered and the droplet size for uniform layer deposition. Inks loaded with particulates are typically misted across the substrate, but to ensure a uniform layer deposition the ink would ideally be deposited in a fine stream. Misted edges that are observed for NOA 74 and NOA 84 in Fig. 6 can be a result of inadequate deposition rate and/or travel speed with respect to the properties of the material being deposited. Another key parameter was the deposition step size, with 50 μm being the optimum step size for depositions in this study. However, to improve deposition quality even further, specifically for NOA 74 and NOA 84, parameters such as atomization rate, travel speed, and step size could be further optimized.

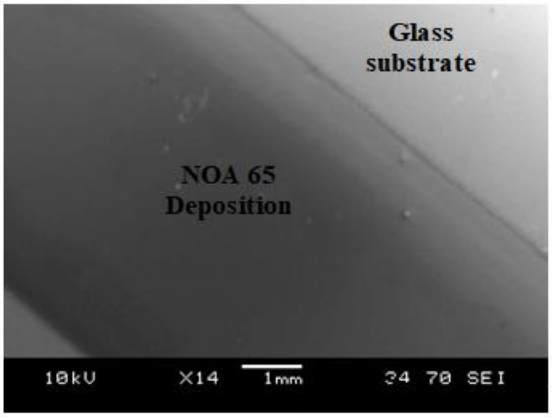

(a)

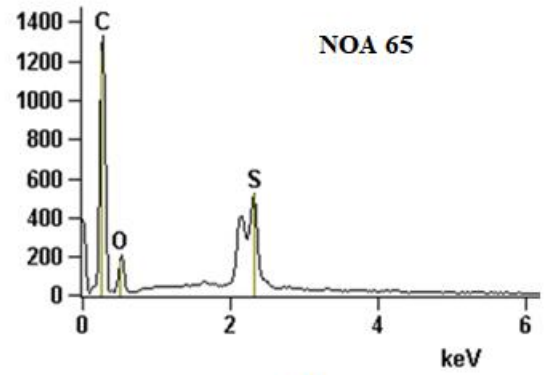

(b)

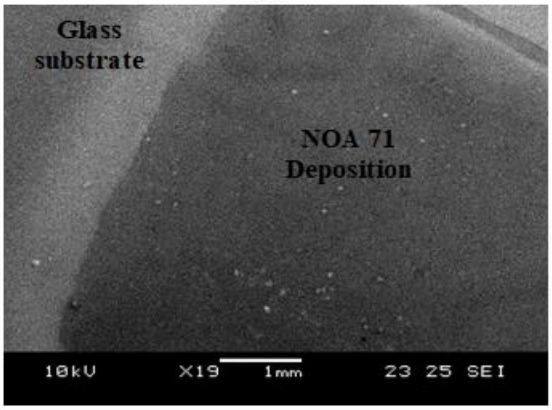

(c)

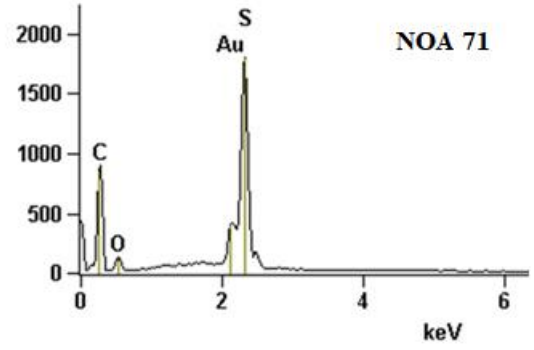

(d)

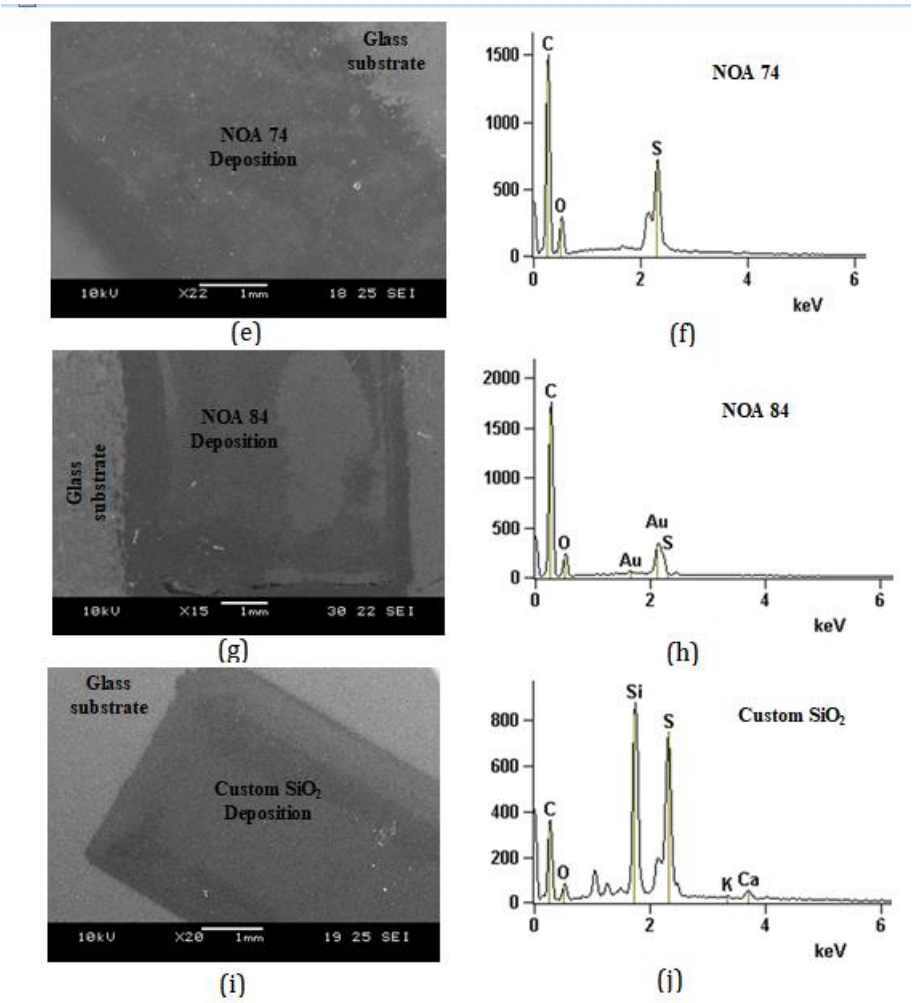

Figure 6 SEM and EDS images representing surface quality and elemental content for each material

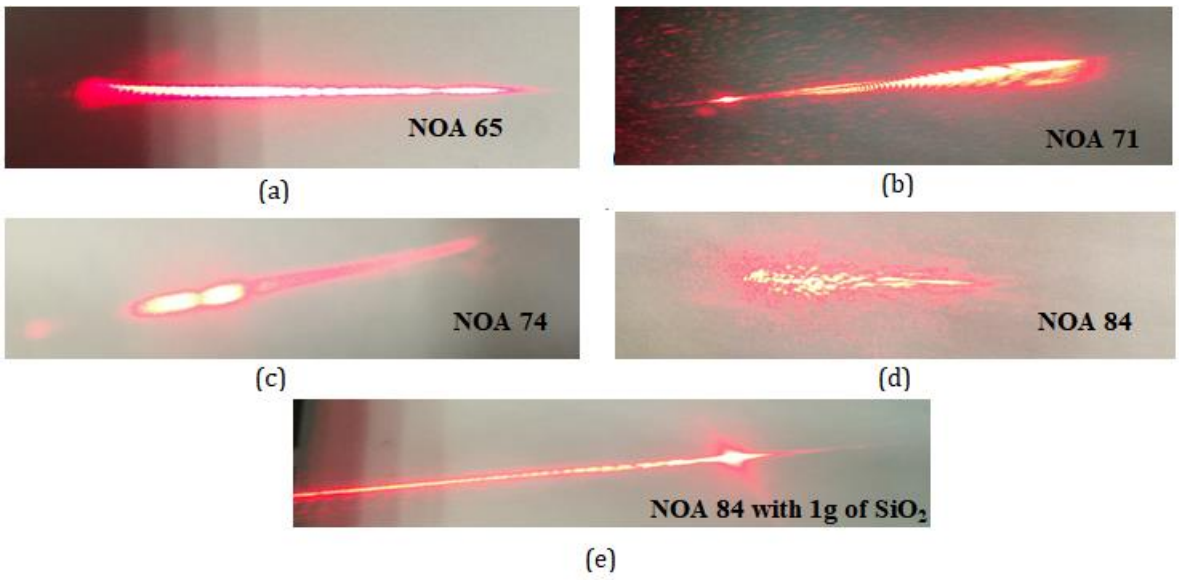

Figure 7 Light reflectivity pattern for each printed material

The pattern of light diffraction in each case is another measurement for inspecting the surface quality of deposited optical-based materials in this study. Figure 7 shows a strong, uniform, and clearly defined light pattern for NOA 65, NOA 71, and custom SiO_2-based ink whereas a dimmed light pattern is shown for NOA 74 and a scattered pattern for NOA 84. The scattered pattern of NOA 84 (Fig. 7d) is a reflection of defect and non-uniformity in the deposited material. Figure 7 shows evidence that high-quality, uniform printed

deposition is important when considering printing of future FBG sensors because even a small mist of side particles can show light defects and variations in measurements.

Conclusion

A non-contact novel printing method using aerosol jet deposition was used to deposit optical-based materials. SiO_2-based ink has been developed for printing with the aerosol jet printer. Gas flow conditions and printing parameters for printing repeatable, dense optical-based materials with excellent edge definition and near bulk properties have been identified. Several limitations in the process needed to be overcome to successfully atomize and effectively deposit each material. System pressure as well as the ability to withstand elevated travel speed became issues for the more viscous materials and less viscous materials, respectively. With less viscous materials, such as NOA 84, elevated speeds were desired to decrease the deposition volume per unit area, whereas high pressure was required to atomize and deliver to the deposition head the more viscous materials, such as NOA 65. A decrease of programming steps and increase in deposition rate produced uniform high-quality depositions. The parameters can be further optimized for lower-viscosity materials that show traits of over-sprayed edges.

While preliminary results from this study show printed deposits with excellent properties and characteristics, a framework for optimization of printing parameters and ink formulation is evident. Furthermore, this study has clearly set some initial guidelines for aerosol jet printing of optical-based materials. The focus in this study was on the process/material property interaction only; the actual printing of sensors on functional components and testing will be discussed in later studies and is beyond the scope of this paper. The preliminary results presented here show that, along with the silica-based ink, the AJP method can be used to fabricate fiber optic sensors. Further, the AJP printing method can eliminate extra manufacturing steps for FBG fibers and provides advantages over traditional fiber manufacturing, which requires fiber pulling then laser writing of the FBG sensors. The FBG sensors can be written directly onto functional components in a variety of systems, which will add significant benefits in the effort to prevent sudden system failures. In future studies, various patterning and formation of FBG grating periods will be explored.

Acknowledgements

The authors acknowledge the help of Mr. Michael Frank (UNT) and Mr. Thomas Jenkins (U.E.S. Corp.) for assisting with the material printing, Mr. Vincent Tondiglia (AFRL-RX) for assisting with UV cure assembly and light reflectivity set-up, Dr. Michael Renn (Optomec Inc.) for valuable discussions and providing input during the process of ink preparation and printing, Dr. Ryan Kohlmeyer (U.E.S. Corp.) and Mr. Aaron Blake (Wright State University) for assisting with the mechanical testing. One of the authors, A. Fortier, acknowledges the Air Force Summer Faculty Fellowship program for fellowship support.

Conflict of Interest: Patent pending related to this work.

References

M. M. Werneck, R. Allil, B. A. Ribeiro, F. V. B. de Nazare, 2013, "Chapter 1: A Guide to Fiber Bragg Grating Sensors", *Intech Open Science Journal*.

Manual by National Instruments, 2016, "Fundamentals of Fiber Bragg Grating (FBG) Optical Sensing".

Hill, K.O., Fujii, Y., Johnson, D. C., and Kawasaki, B. S., 1978, "Photosensitivity in optical fiber waveguides: application to reflection fiber fabrication", *Appl. Phys. Lett.* 32 (10): 647. 24 Current Trends in Short- and Long-Period Fiber Grating

Hill, K.O., 2000, "Photosensitivity in Optical Fiber Waveguides: From Discovery to Commercialization" *IEEE Journal on Selected Topics in Quantum Electronics*, Vol. 6, No. 6, pp. 1186-1189.

Meltz, G., Morey, W. W., and Glenn, W. H., 1989, "Formation of Bragg gratings in optical fibers by a transverse holographic method", *Opt. Lett.* 14 (15): 823.

Werneck, M. M., Allil, R. C. and Ribeiro, B. A., 2012, "Calibration and Operation of a Fiber Bragg Grating Temperature Sensing System in a Grid-Connected Hydrogenerator", *IET Science, Measurement & Technology*

Gwandu, B. A. L. and W. Zhang, W., 2004, "Tailoring the temperature responsivity of fiber Bragg gratings", *Proceedings of IEEESensors*, pp. 1430-1433, Volume 3.

Othonos, A., Kalli, K., 1999, Fiber Bragg Gratings – Fundamentals and Applications in Telecommunications and Sensing, *Artech House*.

Fioria, C., and Devinea, R. A. B., 1985, "Ultraviolet Irradiation Induced Compaction and Photoetching in Amorphous Thermal SiO_2". *MRS Proceedings of the Fall Meeting*, Volume 61.

Riant, I., Borne, S., Sansonetti, P., Poumellec, B., 1995, "Evidence of densification in UV written Bragg gratings in fibres", in Photosensitivity and Quadratic Nonlinearity in Glass Waveguides: Fundamentals and Applications, pp: 52-55, *Postconference Edition, Optical Society of America*.

Jülich, F. and Roths, J., 2009, "Determination of the Effective Refractive Index of Various Single Mode Fibres for Fibre Bragg", *Proceedings of SENSOR+TEST Conference (OPTO-2009), Nürnberg*, pp 119-124.

[Online]. Available at: https://en.wikipedia.org/wiki/Fiber_Bragg_grating Last accessed August 2016.

A. Patil, V.Patil, D.W.Shin, J.Choi, D. Paik, S. Yoon, 2008, "Issues and challenges facing rechargeable thin film lithium batteries", *Materials Research Bulletin*, 43, 1913-1942.

C. R. Liao, D. N. Wang, 2013, "Review of Femtosecond laser fabricated fiber Bragg gratings for high temperature sensing", *Photonic Sensors*, 3: 97.

Klein, J. *et al*. 2015, Additive manufacturing of optically transparent glass. *3D Print. Additive Manuf.* 2, 92–105.

Luo, J., Pan, H. & Kinzel, 2014, E. C. Additive manufacturing of glass. *J. Manuf. Sci. Eng.* 136, 061024.

F. Kotz, K. Arnold, W. Bauer, D. Schild, N. Keller, K. Sachsenheimer, T. M. Nargang, C. Richter, D. Helmer, B. E. Rapp, 2017, "Three-dimensional printing of transparent fused silica glass", *Nature*, 337-339, vol. 544.

Klein, S., Simske S., Parraman C., Walters P., Huson D. & Hoskins S. 2012, 3D Printing of Transparent Glass Technical Report HPL-2012-198, http:// www.hpl.hp.com/ techreports/2012/HPL-2012-198.pdf (Hewlett Packard Labs, 2012).

Marchelli, G., Prabhakar, R., Storti, D. & Ganter, M., 2011, The guide to glass 3D printing: developments, methods, diagnostics and results. *Rapid Prototyping J.* 17, 187–194.

www.optomec.com Last Accessed August 2016.

A.M. Sukeshini, T. Jenkins, P. Gardner, R.M. Miller, T.L. Reitz, 2010, "Investigation of Aerosol Jet Deposition Parameters for Printing SOFC Layers", *Proceedings of the ASME 8th Fuel Cell Science, Engineering and Technology Conference*.

www.Norlandprod.com/adhchart.html Last Accessed August 2016.